Available online at www.eccomasproceedia.org
Eccomas Proceedia UNCECOMP (2023) 94-111

ECCOMAS
Proceedia

UNCECOMP 2023
5th ECCOMAS Thematic Conference on
Uncertainty Quantification in Computational Science and Engineering
M. Papadrakakis, V. Papadopoulos, G. Stefanou (eds.)
Athens, Greece, 12-14 June 2023

INFLUENCE OF THE CHOICE OF THE SEISMIC INTENSITY MEASURE ON FRAGILITY CURVES ESTIMATION IN A BAYESIAN FRAMEWORK BASED ON REFERENCE PRIOR

Antoine Van Biesbroeck[1,2,*], Clément Gauchy[3], Cyril Feau[2] and Josselin Garnier[1]

[1]CMAP, CNRS, École polytechnique, Institut Polytechnique de Paris,
91120 Palaiseau, France
e-mail: antoine.van-biesbroeck@polytechnique.edu, josselin.garnier@polytechnique.edu

[2] Université Paris-Saclay, CEA, Service d'Études Mécaniques et Thermiques,
91191 Gif-sur-Yvette, France
e-mail: cyril.feau@cea.fr

[3] Université Paris-Saclay, CEA, Service de Génie Logiciel pour la Simulation,
91191 Gif-sur-Yvette, France
e-mail: clement.gauchy@cea.fr

Abstract. *Seismic fragility curves are key quantities of the Seismic Probabilistic Risk Assessment studies carried out on industrial facilities. They express the probability of failure of a mechanical structure conditional to a scalar value derived from the seismic ground motion called Intensity Measure (IM). Estimating such curves is a daunting task because for most structures of interest few data are available. For this reason, some methods of the literature rely on the use of the parametric log-normal model coupled with Bayesian approaches for parameter estimation. We are interested in this work in binary datasets (failure or not failure) and we investigate the influence of the choice of the prior and of the IM – Peak Ground Acceleration vs. Pseudo Spectral Acceleration – on the convergence of the estimates for a given seismic scenario. We show that Bayesian fragility curve estimation results based on Jeffreys' prior outperform the ones based on classical priors whatever the IM. We also show that, when an IM is more correlated to the structural response, the differences between the results obtained with the different priors are less marked. They testify to the fact that an IM more correlated to the response of the structure induces a lower variability of the estimate of the median of the log-normal model. This is not the case for the log standard deviation whose estimate is affected by samples which are more degenerate with this kind of IM, namely which are partitioned into two disjoint subsets when classified according to IM values: the subset for which there is no failure and the other one for which there is failure, these two subsets possibly being present in the same sample or separately. Such degeneracy affects all methods to varying degrees, but with Jeffreys' prior the results are clearly better, attesting to its robustness against such inevitable situations in practice.*

Keywords: Bayesian analysis, Fragility curves, Reference prior, Jeffreys prior, Seismic Probabilistic Risk Assessment

ISSN:2623-3339 © 2023 The Authors. Published by Eccomas Proceedia.
Peer-review under responsibility of the organizing committee of UNCECOMP 2023.
doi: 10.7712/120223.10327.19899

1 Introduction

Seismic fragility curves are key quantities of the Seismic Probabilistic Risk Assessment (SPRA) studies carried out on mechanical structures. They were introduced in the 1980s for safety studies of nuclear facilities (see e.g. [1–5]). They express the probability of failure of the mechanical structure conditional to a scalar value derived from the seismic ground motions – called Intensity Measure (IM) – such as the Peak Ground Acceleration (PGA) or the Pseudo-Spectral Acceleration (PSA) for a fixed frequency and damping. In practice, various data sources can be exploited to estimate fragility curves, namely: expert judgments supported by test data [1–3, 6], experimental data [3, 7, 8], results of damage collected on existing structures that have been subjected to an earthquake [9–11] and analytical results given by more or less refined numerical models using artificial or real seismic excitations (see e.g. [12–17]). Parametric fragility curves were historically introduced in the SPRA framework because their estimates require small sample sizes. The log-normal model has since become the most widely used model (see e.g. [9–22]). Several strategies can be implemented to fit the median, α, and the log standard deviation, β, of the model. Some of them are compared in [10] highlighting advantages and disadvantages. When the data is binary – i.e. when it indicates failure or not – [10] recommended maximum likelihood estimation (MLE). When the data are independent, the bootstrap technique can be used to obtain confidence intervals relating to the size of the sample considered (e.g. [9, 12, 13]).

Among the various other methods not mentioned in this short introduction, the Bayesian framework has recently become increasingly popular in seismic fragility analysis (see e.g. [7, 16, 22–28]). It actually allows to solve irregularity issues encountered in the estimation of the parametric fragility curves. MLE-based methods can indeed lead to unrealistic or degenerate fragility curves such as unit step functions when the data availability is sparse. Those problems are especially encountered when resorting to complex and detailed modeling due to the calculation burden or when dealing with tests performed on shaking tables, etc. In earthquake engineering, Bayesian inference is often used to update log-normal fragility curves obtained beforehand by various approaches, by assuming independent distributions for the prior values of α and β such as log-normal distributions (see e.g. [11, 16, 22, 25, 26]).

This work follows the one presented in [29] which deals with Bayesian problems in which only few binary data are available. Using the reference prior theory as a support, the authors have proposed an objective approach to choose the prior and to simulate a posteriori fragility curves. This approach led to the Jeffreys' prior and the authors have shown the robustness and advantages of the Jeffreys' prior in terms of regularization (no degenerate estimations) and stability (no outliers of the parameters) for fragility curves estimation. Since this prior depends only on the characteristics of the ground motion – the distribution of the IM of interest – its calculation is then suitable for any equipment of an industrial installation subjected to the same seismic hazard. So, in this work, we are interested in the influence of the choice of the IM – PGA vs. PSA – on the convergence of the estimates, for a given magnitude (M) - source-to-site distance (R) scenario and a given mechanical structure.

The paper is organized as follows. Section 2 presents the statement of the problem from the Bayesian viewpoint. A review of the objective prior theory is presented in section 3. The principal achievements of [29] on which we rely are summarized in section 4. Section 5 is dedicated to reviewing estimation tools and benchmarking metrics used to support comparisons with classical approaches of the literature. They are implemented in section 6 on a case study, a piping system. A conclusion is proposed in section 7.

2 Bayesian problem

A log-linear probit model is often used to approximate fragility curves. In this model the probability of failure given the IM takes the following form:

$$P_f(a) = \mathbb{P}(\text{`failure'}|\text{IM} = a) = \Phi\left(\frac{\log a - \log \alpha}{\beta}\right), \tag{1}$$

where $\alpha, \beta \in (0, +\infty)$ are the two model parameters and Φ is the cumulative distribution function of a standard Gaussian variable. In the following we denote $\theta = (\alpha, \beta)$. In the Bayesian point of view θ is considered as a random variable [30]. Its probability density function is denoted by π and called the prior, it is supposed to be defined on a set $\Theta \subset (0, +\infty)^2$.

The statistical model consists in the observations of independent realizations $(a_1, z_1), \ldots, (a_k, z_k) \in \mathcal{A} \times \{0, 1\}$, $\mathcal{A} \subset [0, \infty)$, k being the data-set size. For the ith seismic event, a_i is its observed IM and z_i is the observation of a failure (z_i is equal to one if failure has been observed during the ith seismic event and it is equal to zero otherwise). The joint distribution of the pair (a, z) conditionally to θ has the form:

$$p(a, z|\theta) = p(a)p(z|a, \theta), \tag{2}$$

where $p(a)$ denotes the distribution of the IM and $p(z|a, \theta)$ is a Bernoulli distribution whose parameter (the probability of failure) depends on a and θ as expressed by equation (1). The product of the conditional distributions $p(z_i|a_i, \theta)$ is the likelihood of the model:

$$\ell_k(\mathbf{z}|\mathbf{a}, \theta) = \prod_{i=1}^{k} p(z_i|a_i, \theta) = \prod_{i=1}^{k} \Phi\left(\frac{\log \frac{a_i}{\alpha}}{\beta}\right)^{z_i} \left(1 - \Phi\left(\frac{\log \frac{a_i}{\alpha}}{\beta}\right)\right)^{1-z_i}, \tag{3}$$

denoting $\mathbf{a} = (a_i)_{i=1}^k$, $\mathbf{z} = (z_i)_{i=1}^k$. The *a posteriori* distribution of θ can be computed by Bayes theorem. The resulting posterior distribution is:

$$p(\theta|\mathbf{a}, \mathbf{z}) = \frac{\ell_k(\mathbf{z}|\mathbf{a}, \theta)\pi(\theta)}{\int_\Theta \ell_k(\mathbf{z}|\mathbf{a}, \theta')\pi(\theta')d\theta'}. \tag{4}$$

3 Reference prior theory

To choose a non-subjective prior, in [29] is considered the criterion introduced by Bernardo [31] to define the so-called reference prior. It consists in choosing the prior that maximizes the mutual information indicator $I(\pi|k)$ which expresses the information provided by the data to the posterior, relatively to the prior. In other words, this criterion seeks the prior that maximizes the "learning" capacity from observations. The mutual information indicator is defined by:

$$I(\pi|k) = \int_{(\mathcal{A}\times\{0,1\})^k} KL(p(\cdot|\mathbf{a}, \mathbf{z})||\pi)p(\mathbf{a}, \mathbf{z}) \prod_{l=1}^{k} \lambda(da_l, dz_l), \tag{5}$$

where $p(\mathbf{a}, \mathbf{z}) = \int_\Theta \ell_k(\mathbf{z}|\mathbf{a}, \theta') \prod_{l=1}^k p(a_l)\pi(\theta')d\theta'$ and the reference measure $\lambda(da, dz)$ is the product of the Lebesgue measure over $\mathcal{A}$ w.r.t. a and the discrete measure $\delta_0 + \delta_1$ over $\{0, 1\}$ w.r.t. z: we have $\int_{\mathcal{A}\times\{0,1\}} \psi(a, z)\lambda(da, dz) = \int_{\mathcal{A}} \psi(a, 0)da + \int_{\mathcal{A}} \psi(a, 1)da$ for any test function ψ. The indicator (5) is based on the Kullback-Leibler divergence between the posterior and the prior, which is known to numerically express this idea of the information provided by one distribution to another one:

$$KL(p||\pi) = \int_\Theta p(\theta) \log \frac{p(\theta)}{\pi(\theta)} d\theta. \tag{6}$$

A suitable definition of a reference prior is suggested in the literature as the solution of an asymptotic optimization of this mutual information metric [32, 33]. It has been proved that, under some mild assumptions which are satisfied in our framework, the Jeffreys' prior defined by

$$J(\theta) \propto \sqrt{|\det \mathcal{I}^k(\theta)|}, \tag{7}$$

is the reference prior, with $\mathcal{I}^k$ being the Fisher information matrix:

$$\mathcal{I}(\theta)^k_{i,j} = -\int_{(\mathcal{A}\times\{0,1\})^k} \ell_k(\mathbf{z}|\mathbf{a},\theta) \frac{\partial^2 \log \ell_k(\mathbf{z}|\mathbf{a},\theta)}{\partial\theta_i \partial\theta_j} \prod_{l=1}^k p(a_l)\lambda(da_l, dz_l). \tag{8}$$

The property $\mathcal{I}(\theta)^k = k\mathcal{I}(\theta)$ (with $\mathcal{I}(\theta) = \mathcal{I}(\theta)^1$) makes J independent of k, as its definition only stands up to a multiplicative constant. The Jeffreys' prior is already well known in Bayesian theory for being invariant by a reparametrization of the statistical model [34]. This property is essential as it makes the choice of the model parameters θ without any incidence on the resulting posterior.

4 Jeffreys' prior construction

4.1 Jeffreys' prior calculation

In a first step, we compute the Fisher information matrix $\mathcal{I}(\theta)$ in our model. Here, $\theta = (\alpha, \beta) \in \Theta$ and

$$\mathcal{I}(\theta)_{i,j} = -\int_{\mathcal{A}\times\{0,1\}} p(z|a,\theta) \frac{\partial^2 \log p(z|a,\theta)}{\partial\theta_i \partial\theta_j} p(a)\lambda(da, dz) \tag{9}$$

for $i, j \in \{1, 2\}$, with $p(z|a,\theta) = \ell_1(z|a,\theta)$ being the likelihood expressed in equation (3), i.e.

$$\log p(z|a,\theta) = z \log \Phi\left(\frac{\log a - \log\alpha}{\beta}\right) + (1-z)\log\left(1 - \Phi\left(\frac{\log a - \log\alpha}{\beta}\right)\right). \tag{10}$$

From [29], the information matrix $\mathcal{I}(\theta)$ is given by:

$$\mathcal{I}(\theta) = \begin{pmatrix} \frac{1}{\alpha^2\beta^2}(A_{01} + A_{02}) & \frac{1}{\alpha\beta^3}(A_{11} + A_{12}) \\ \frac{1}{\alpha\beta^3}(A_{11} + A_{12}) & \frac{1}{\beta^4}(A_{21} + A_{22}) \end{pmatrix}, \tag{11}$$

with

$$\begin{aligned} A_{01} &= \int_\mathcal{A} \frac{\Phi'(\gamma(a))^2}{\Phi(\gamma(a))} p(a)da, & A_{02} &= \int_\mathcal{A} \frac{\Phi'(\gamma(a))^2}{\Phi(-\gamma(a))} p(a)da, \\ A_{11} &= \int_\mathcal{A} \log\frac{a}{\alpha} \frac{\Phi'(\gamma(a))^2}{\Phi(\gamma(a))} p(a)da, & A_{12} &= \int_\mathcal{A} \log\frac{a}{\alpha} \frac{\Phi'(\gamma(a))^2}{\Phi(-\gamma(a))} p(a)da, \\ A_{21} &= \int_\mathcal{A} \log^2\frac{a}{\alpha} \frac{\Phi'(\gamma(a))^2}{\Phi(\gamma(a))} p(a)da, & A_{22} &= \int_\mathcal{A} \log^2\frac{a}{\alpha} \frac{\Phi'(\gamma(a))^2}{\Phi(-\gamma(a))} p(a)da, \end{aligned} \tag{12}$$

and $\gamma(a) = \beta^{-1}\log\frac{a}{\alpha}$.

The Jeffreys' prior is known to be improper in numerous common cases (i.e. it cannot be normalized as a probability). In the present case, its asymptotic behavior is computed for

different limits of $\theta = (\alpha, \beta)$ in [29] which shows that it is indeed improper. This characteristic is not an issue, as our work focuses on the posterior which is proper as proved in [29]. This property is essential as MCMC algorithms would not make any sense if the posterior were improper.

4.2 Practical implementation

In this work we use 10^5 artificial seismic signals generated using the stochastic generator defined in [35] and implemented in [36] from 97 real accelerograms selected in the European Strong Motion Database for $5.5 \leq \mathrm{M} \leq 6.5$ and $\mathrm{R} < 20$ km. Enrichment is not a necessity in the Bayesian framework – especially if a sufficient number of real signals is available – but it allows comparisons with the reference method of Monte-Carlo for simulation-based approaches as well as comparative studies of performance. For instance, Figure 1 shows that the synthetic signals have the same PGA distribution as the real ones as well as the PSA which is here calculated at 5 Hz for 1% damping ratio (see section 6 for justification). Moreover, the asymptotic expansions provided in [29] give complementary and essential insight into the Jeffreys' prior. They evince that its behavior in α is similar to that of a log-normal distribution having the same median as that of the IM with a variance which is the sum of the variance of the IM and of a term which depends on β. Figure 1 illustrates also this result for the two IMs.

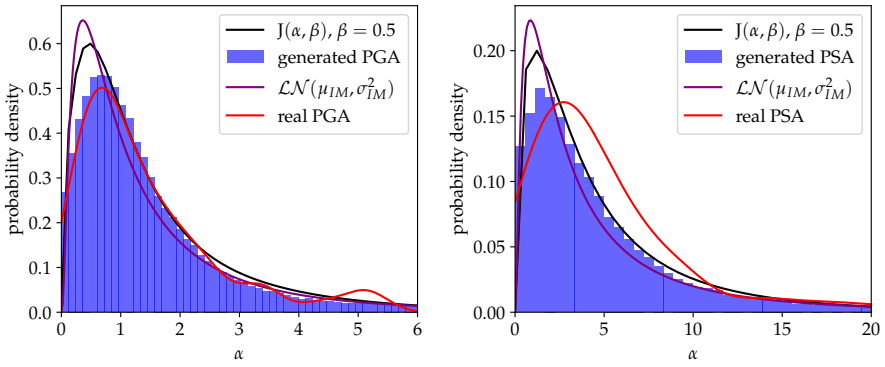

(a) PGA (b) PSA

Figure 1: Comparison of a sectional view of the Jeffreys' prior w.r.t. α (black) with the approximated distributions of real accelerograms via Gaussian kernel estimation (red), the histograms of the generated signals (blue) and the log-normal approximations (purple) for both IMs.

In practice, due to the use of Markov Chain Monte Carlo (MCMC) methods to sample the *a posteriori* distribution, the prior must be evaluated (up to a multiplicative constant) many times in the calculations. Because of its computational complexity due to the integrals to be computed, we performed evaluations of the prior on an experimental design based on a fine-mesh grid of Θ (here $(0, +\infty)^2$) and to build an interpolated approximation of the Jeffreys' prior from this design. This strategy is more suitable for our numerical applications and very tractable because the domain Θ is only two-dimensional. Figure 2 shows plots of the Jeffreys' priors.

5 Estimation tools, competing approaches and benchmarking metrics

In this section, we first present the Bayesian estimation tools and the Monte-Carlo reference method to which we refer to evaluate the relevance of the log-normal model. Then, to evaluate

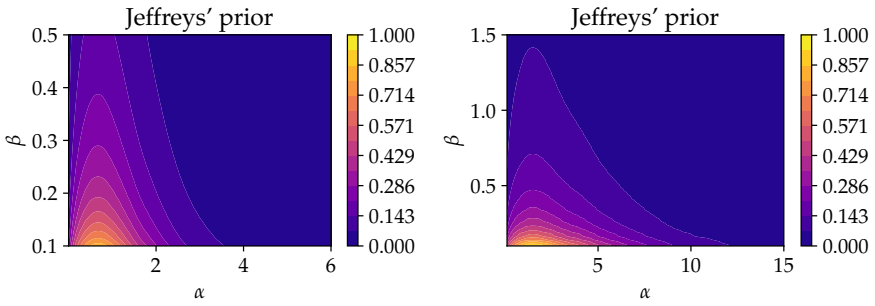

(a) PGA (b) PSA

Figure 2: The Jeffreys' priors calculated from PGA and PSA on subdomains of $\Theta = (0, +\infty)^2$.

the performance of the Jeffreys' prior, we present two competing approaches that we implement. On the one hand, we apply the MLE method widely used in literature, coupled with a bootstrap technique. On the other hand, we apply a Bayesian technique implemented with the prior introduced by Straub and Der Kiureghian [11]. Performance evaluation metrics are then defined.

5.1 Fragility curves estimations via Monte-Carlo

We assume that a validation data-set $(\mathbf{a}^{\mathrm{MC}}, \mathbf{z}^{\mathrm{MC}}) = ((a_i^{\mathrm{MC}})_{i=1}^{N^{\mathrm{MC}}}, (z_i^{\mathrm{MC}})_{i=1}^{N^{\mathrm{MC}}})$ is available. For nonparametric estimations, good candidates are Monte-Carlo (MC) estimators which estimate the expected number of failures locally w.r.t. the IM. We first need to define a subdivision of the IM values and to estimate the failure probability on each of the sub-intervals. Regular subdivisions are not appropriate because the observed IMs are not uniformly distributed. We follow the suggestion by Trevlopoulos et al. [21] to take clusters of the IM using K-means. Given such N_c clusters $(K_j)_{j=1}^{N_c}$, the Monte-Carlo fragility curve estimated at the centroids $(c_j)_{j=1}^{N_c}$ is expressed as

$$P_f^{\mathrm{MC}}(c_j) = \frac{1}{n_j} \sum_{i,\, a_i^{\mathrm{MC}} \in K_j} z_i^{\mathrm{MC}}, \tag{13}$$

where $n_j = \mathrm{Card}(i,\, a_i^{\mathrm{MC}} \in K_j)$ is the size of cluster K_j. An asymptotic confidence interval for this estimator can also be derived using its Gaussian approximation. It is accepted that a MC-based fragility curve is a reference curve because it is not based on any assumption.

5.2 Fragility curves estimations in the Bayesian framework

From equation (4) *a posteriori* samples of θ can be obtained by MCMC methods. We have implemented an adaptive Metropolis-Hastings (M-H) algorithm with Gaussian transition kernel and covariance adaptation [37]. Such an algorithm allows for simulations from a probability density known up a multiplicative constant. The *a posteriori* samples of θ can be used to define credible intervals for the log-normal estimates of the fragility curves.

5.3 Competing approaches for performance evaluation

Multiple MLE by bootstrapping. The best known parameter estimation method is the MLE, defined as the maximal argument of the likelihood derived from the observed data:

$$\hat{\theta}_k^{\mathrm{MLE}} = \arg\max_{\theta \in \Theta} \ell_k(\mathbf{z}|\mathbf{a}, \theta). \tag{14}$$

A common method for obtaining a wide range of θ estimates is to compute multiple MLE by bootstrapping. Denoting the data-set size by k, bootstrapping consists in doing L independent draws with replacement of k items within the data-set. Those lead to L different likelihoods from the k initial observations, and so to L values of the estimator which can be averaged. In the context of fragility curves, this method is widespread (see e.g. [9, 10, 13, 38, 39]). The convergence of the MLE and the relevance of this method is stated in [40]. Nevertheless the bootstrap method is often limited by the irregularity of the results for small values of k (see e.g. [6]). In this context, the L values of θ are used to define confidence intervals for the log-normal estimates of the fragility curves.

Prior suggested by Straub and Der Kiureghian [11]. The prior suggested by Straub and Der Kiureghian – called SK's prior – is defined as the product of a normal distribution for $\ln(\alpha)$ and the improper distribution $1/\beta$ for β, namely:

$$\pi_{SK}(\theta) \propto \frac{1}{\alpha\beta} \exp\Big(- \frac{(\log\alpha - \mu)^2}{2\sigma^2} \Big). \tag{15}$$

In [11] the parameters μ and σ of the log-normal distribution are chosen to generate a non-informative prior. For a fair comparison with the approach proposed in this paper, we decided to choose μ and σ being equal to the mean and the standard deviation of the logarithm of the IM, whether the PGA or the PSA. This choice is consistent with the fact that the Jeffreys' prior is similar to a log-normal distribution with these parameters (see Figure 1). The prior $\pi_{SK}(\theta)$ is plotted in Figure 3 for the two IMs.

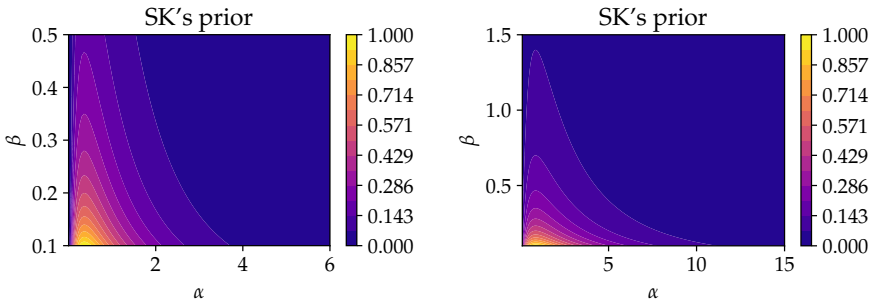

(a) PGA (b) PSA

Figure 3: Prior suggested by Straub and Der Kiureghian [11] scaled on log-normal estimations of the IM distributions.

An analysis of the posterior which results from SK's prior is given in [29]. It shows that the posterior is improper. This statement jeopardizes the validity of *a posteriori* simulations using MCMC methods if we consider the whole domain $\Theta = (0, +\infty)^2$. This issue is nevertheless manageable with the consideration of a truncation w.r.t. β.

5.4 Benchmarking metrics

In order to evaluate the performance of the proposed approach, we consider two quantitative metrics which can be calculated for each of the methods described in section 5.3. We consider the sample $(\mathbf{a}, \mathbf{z})$. We denote by $a \mapsto P_f^{|\mathbf{a},\mathbf{z}}(a)$ the random process defined as the fragility curve conditional to the sample (the probability distribution of $P_f^{|\mathbf{a},\mathbf{z}}(a)$ is inherited from the a

posteriori distribution of θ). For each value a the r-quantile of the random variable $P_f^{|\mathbf{a},\mathbf{z}}(a)$ is denoted by $q_r^{|\mathbf{a},\mathbf{z}}(a)$. We define:

- The conditional quadratic error:

$$\mathcal{E}^{Q|\mathbf{a},\mathbf{z}} = \mathbb{E}\big[\|P_f^{|\mathbf{a},\mathbf{z}} - P_f^{\mathrm{MLE}}\|_{L^2}^2 |\mathbf{a},\mathbf{z}\big], \qquad \|P\|_{L^2}^2 = \frac{1}{A_{\max}}\int_0^{A_{\max}} P(a)^2 da. \tag{16}$$

  P_f^{MLE} stands for the log-normal estimate of the fragility curve obtained by MLE with all the database available. We further check that this estimate is close to the reference curve obtained by MC.

- The conditional width of the $1-r$ credible zone for the fragility curve:

$$\mathcal{S}^{r|\mathbf{a},\mathbf{z}} = \|q_{1-r/2}^{|\mathbf{a},\mathbf{z}} - q_{r/2}^{|\mathbf{a},\mathbf{z}}\|_{L^2}^2. \tag{17}$$

To estimate such variables, we simulate a set of L fragility curves $(P_f^{\theta_i|\mathbf{a},\mathbf{z}})_{i=1}^L$ where $(\theta_i)_{i=1}^L$ is a sample of the *a posteriori* distribution of the model parameters obtained by MCMC. The empirical quantiles $\hat{q}_r^{\theta_{i=1}^L|\mathbf{a},\mathbf{z}}(a)$ of $(P_f^{\theta_i|\mathbf{a},\mathbf{z}}(a))_{i=1}^L$ are approximations of the quantiles $q_r^{|\mathbf{a},\mathbf{z}}(a)$ of the random variable $P_f^{|\mathbf{a},\mathbf{z}}(a)$. We derive:

- The approximated conditional quadratic error:

$$\hat{\mathcal{E}}_L^{Q|\mathbf{a},\mathbf{z}} = \frac{1}{L}\sum_{i=1}^{L} \|P_f^{\theta_i|\mathbf{a},\mathbf{z}} - P_f^{\mathrm{MLE}}\|_{L^2}^2. \tag{18}$$

- The approximated conditional width of the $1-r$ credible zone for the fragility curve:

$$\hat{\mathcal{S}}_L^{r|\mathbf{a},\mathbf{z}} = \|\hat{q}_{1-r/2}^{\theta_{i=1}^L|\mathbf{a},\mathbf{z}} - \hat{q}_{r/2}^{\theta_{i=1}^L|\mathbf{a},\mathbf{z}}\|_{L^2}^2. \tag{19}$$

The normalized L^2 norms are normalized integrals over $a \in [0, A_{\max}]$ which are approximated numerically using Simpson's interpolation on a regular subdivision $0 = A_0 < \cdots < A_p = A_{\max}$. In the forthcoming section we use $A_0 = 0$, $A_{\max} = 24\,\mathrm{m/s^2}$ for the PGA and $A_{\max} = 50\,\mathrm{m/s^2}$ for the PSA with $p = 200$.

For the MLE with bootstrapping, we can define a conditional quadratic error as in equation (18) and conditional width of the $1-r$ confidence interval as in equation (19) using a bootstrapped sample $(\theta_i)_{i=1}^L$.

6 Numerical application

6.1 Presentation of the piping system

This case study concerns a piping system that is a part of a secondary line of a French Pressurized Water Reactor. This piping system was studied, experimentally and numerically, as part of the ASG program [41]. Figure 4 shows a view of the mock-up mounted on the shaking table Azalee of the EMSI laboratory of CEA/Saclay whereas the Finite Element Model (FEM) – based on beam elements – is shown in Figure 4-right. The latter has been implemented with the homemade FE code CAST3M [42] and has been validated via an experimental campaign.

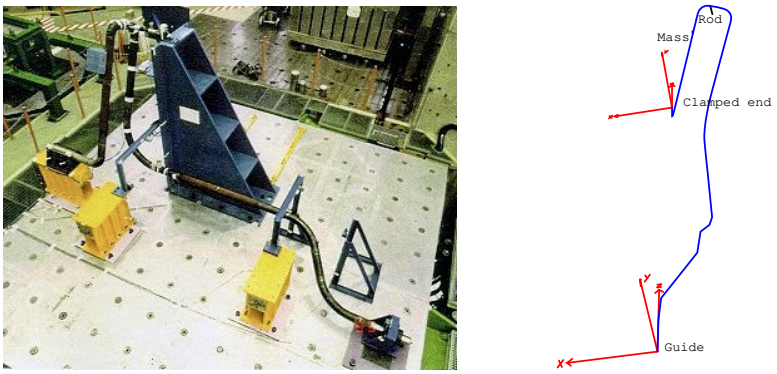

(a) (b)

Figure 4: (a) Overview of the piping system on the Azalee shaking table and (b) Mock-up FEM.

One end of the mock-up is clamped whereas the other is supported by a guide in order to prevent the displacements in the X and Y directions. Additionally, a rod is placed on the top of the specimen to limit the mass displacements in the Z direction (see Figure 4-right). In the tests, the excitation is only imposed in the X direction. For this study, the artificial signals are filtered by a fictitious 2% damped linear single-mode building at 5 Hz, the first eigenfrequency of the 1% damped piping system. As failure criterion, we consider excessive out-of-plane rotation of the elbow located near the clamped end of the mock-up, as recommended in [43]. The critical rotation considered here is equal to $1.6°$. This is the level quantile 90% of a sample of size 10^5 of numerical simulations carried out assuming a linear behavior of the piping system. A linear behavior is considered to simply highlight the influence of the choice of IM. Indeed we use on the one hand the PGA and on the other hand the PSA of the initial set of synthetic signals (i.e not filtered signals), calculated at 5 Hz and 1% damping ratio. Figure 5 shows that the PSA is clearly better correlated with the response of the structure than the PGA.

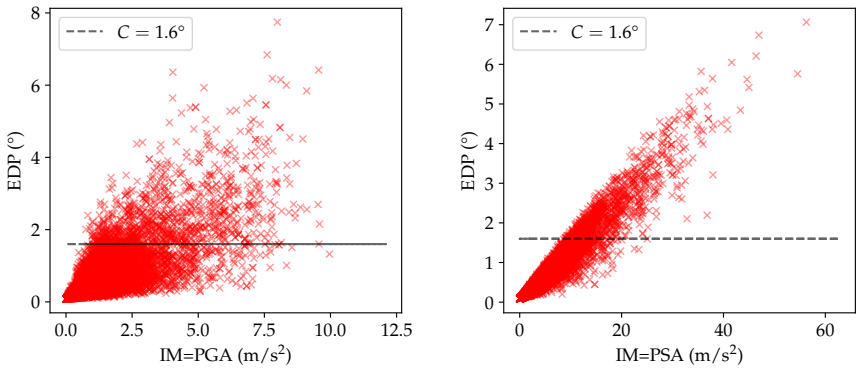

(a) PGA (b) PSA

Figure 5: Scatter plots of the out-of-plane elbow rotation as a function of (a) PGA and (b) PSA for a linear seismic behavior of the piping system.

For the two IMs, Figure 6 shows the comparisons between the reference MC-based fragility curves P_f^{MC} and their log-normal estimates P_f^{MLE}, both estimated via 10^5 simulations results.

In both cases, the log-normal fragility curves are good approximations of the reference ones.

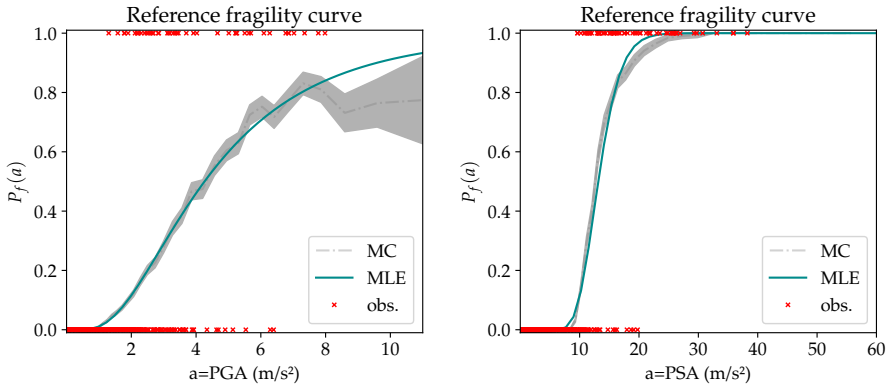

(a) PGA (b) PSA

Figure 6: Reference fragility curves P_f^{MC} compared with P_f^{MLE} computed using the full data-set generated (10^5 items) for the two IMs. The red crosses represent the observations.

6.2 Results and discussion

Figures 7 and 8 present the results for the PGA and the PSA as IM respectively. Figures 7-(a) and (b) (resp. figures 8-(a) and (b)) show the metrics $\hat{\mathcal{E}}_{L,R}^{Q|\mathbf{a}^{(j)},\mathbf{z}^{(j)}}$, $\hat{\mathcal{S}}_{L,R}^{r|\mathbf{a}^{(j)},\mathbf{z}^{(j)}}$, $j \in \{1,\dots,m\}$, $R \in \{$'MLE', 'SK', 'Jeffreys'$\}$, $L = 5000$, $1-r = 95\%$ for any k varying from 15 to 100 and $m = 200$. Figures 7-(c) and 8-(c) present examples of fragility curves credibility (or confidence for the MLE) intervals for the three methods introduced in section 5.3 for $k = 30$, in comparison with P_f^{MLE}. Those are computed from generated pairs (α, β) whose scatter plots are presented in figures 7-(d) and 8-(d).

In addition, to get a better overview on the results, we also show in figure 9 the coefficients of variation of the two parameters (α, β) as a function of both IM and k.

Generally speaking, theses results show, as expected, that when the IM is more correlated to structural response, the differences between the methods are less marked, although in detail there may be some small differences depending on the sample size. Figure 9 clearly shows that an IM more correlated to the response of the structure induces a lower variability of the estimate of the median of the log-normal model. This is not the case for the log standard deviation whose estimate is affected by samples which are more degenerate with this kind of IM, namely which are partitioned into two disjoint subsets when classified according to IM values: the subset for which there is no failure and the other one for which there is failure, these two subsets possibly being present in the same sample or separately. Such degeneracy affects all methods to varying degrees but in all cases, the Jeffreys' prior outperforms SK's prior and MLE.

Whereas the SK's prior is calibrated to look like the Jeffreys' prior, figures 7-(d) and 8-(d) show that many outliers – i.e. large values of the pair (α, β) – are simulated with the SK's prior. These values explain that the credible intervals of the fragility curves and the metrics $\hat{\mathcal{E}}_{L,R}^{Q|\mathbf{a}^{(j)},\mathbf{z}^{(j)}}$ and $\hat{\mathcal{S}}_{L,R}^{r|\mathbf{a}^{(j)},\mathbf{z}^{(j)}}$ are larger with the SK's prior. This observation is both supported by figure 9 and by the calculations provided in [29] regarding β. Indeed, in [29] is shown a better convergence of the Jeffreys' prior toward 0 when $\beta \longrightarrow \infty$. This better asymptotic behavior results in posteriors which happen to give a lower probability to outlier points – phenomenon

particularly noticeable when the data-set is small – as well as to the weight of the likelihood within the posterior.

Although the intervals compared – that of the Bayesian framework and that of the MLE – are not of the same nature – credible interval for the first *versus* confidence interval for the second – these results clearly illustrate the advantage of the Bayesian framework over the MLE for small samples. Indeed, irregularities appear in the MLE method that are characterized by null estimates of β, which result (i) in important coefficient of variation of β (figure 9) and (ii) in "vertical" confidence intervals on fragility curves estimations (figures 7-(c) and 8-(c)). When few failures are observed, some samples – both initial and bootstrapped samples – are degenerate, as explained earlier. As no prior is considered in MLE, the likelihood can then be easily maximized with $\beta = 0$. In [29], it is proven that such scenarios result in degenerate likelihood. This last statement is perceived better through figures 7-(d) and 8-(d). The zero-degenerate β values that result from the MLE appear clearly. This leads to a confidence interval generally larger than the credible intervals, except for very small values of k ($k \simeq 20$) when the IM is well correlated with the response of the structure, i.e. with the PSA. Indeed, with a perfect IM - which only exists if we know the structural response itself - the fragility curve is degenerate and has the form of a unit step function. The associated confidence interval is of null size, since in this case it does not require any sample to estimate the fragility curve. So, although apparently better, such confidence intervals are meaningless since they are based on degenerate estimates.

As proven in [29], in the Bayesian context, the same degenerate samples also produce degeneracy but "less marked" than for MLE, as the phenomena is regularized by the prior distribution. As the results show, this affects SK's prior more than Jeffreys' one. This is observed, in particular, when the IM is very well correlated with the response of the structure since, in this case, it is more probable to obtain this kind of degenerate samples. Therefore, when $k < 40$, the credible intervals are slightly larger with the PSA than with the PGA. This is also confirmed by the results shown in figure 9. So, counter-intuitively, when very few data are available, a less well-specified problem from the point of view of the choice of the IM leads to better convergences of the estimates, because it produces fewer degenerate samples. However, this remains confined to very small sample sizes and therefore cannot be considered representative. Note that, in all cases, the Jeffreys' prior outperforms SK's prior and MLE.

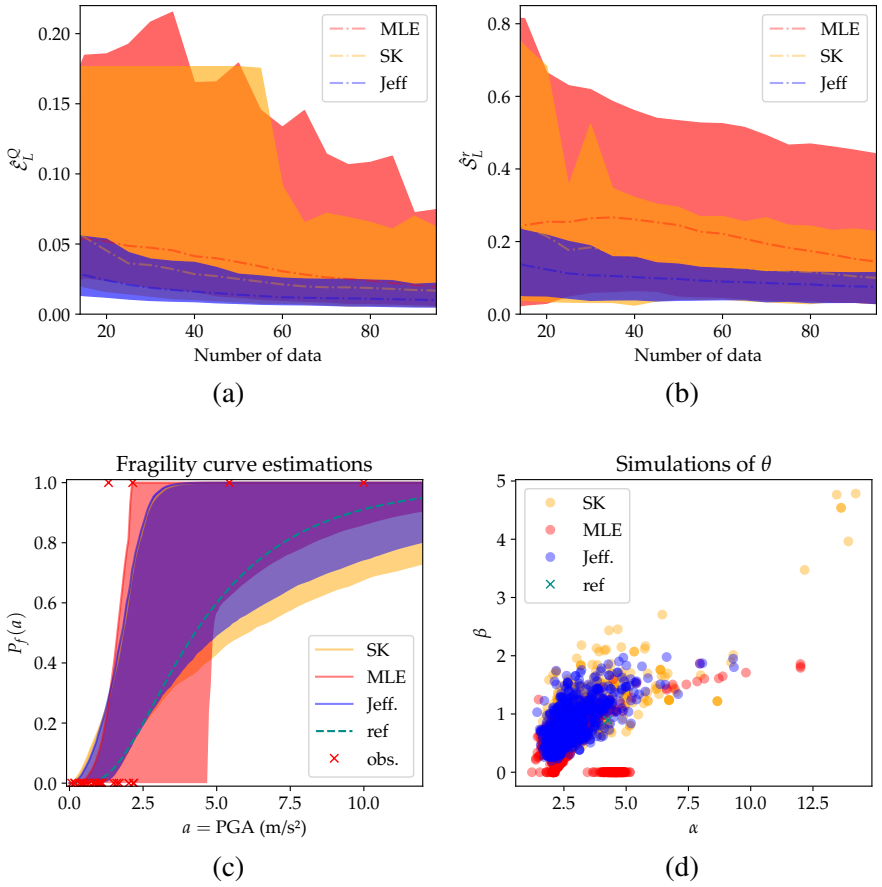

Figure 7: (a) the dashed lines plot the quadratic errors as a function of the number of data k and the shaded areas show their confidence intervals; (b) the dashed lines plot the widths of the 95% credible intervals (for Bayesian estimation) or confidence intervals (for MLE) and the shaded areas show their confidence intervals; (c) the shaded areas show the 95% credible (for Bayesian estimation) or confidence (for MLE) intervals resulting from a total of 5000 simulations of θ using the three methods considered for $k = 30$; (d) scatter plots of the generated θ to estimate the fragility curves for the three methods (500 points from the 5000 $\theta = (\alpha, \beta)$ generated are plotted); the green cross in (d) plot θ^{MLE} which is used for the computation of P_f^{MLE}, plotted as a green dashed line in (c). Here the PGA is used as IM.

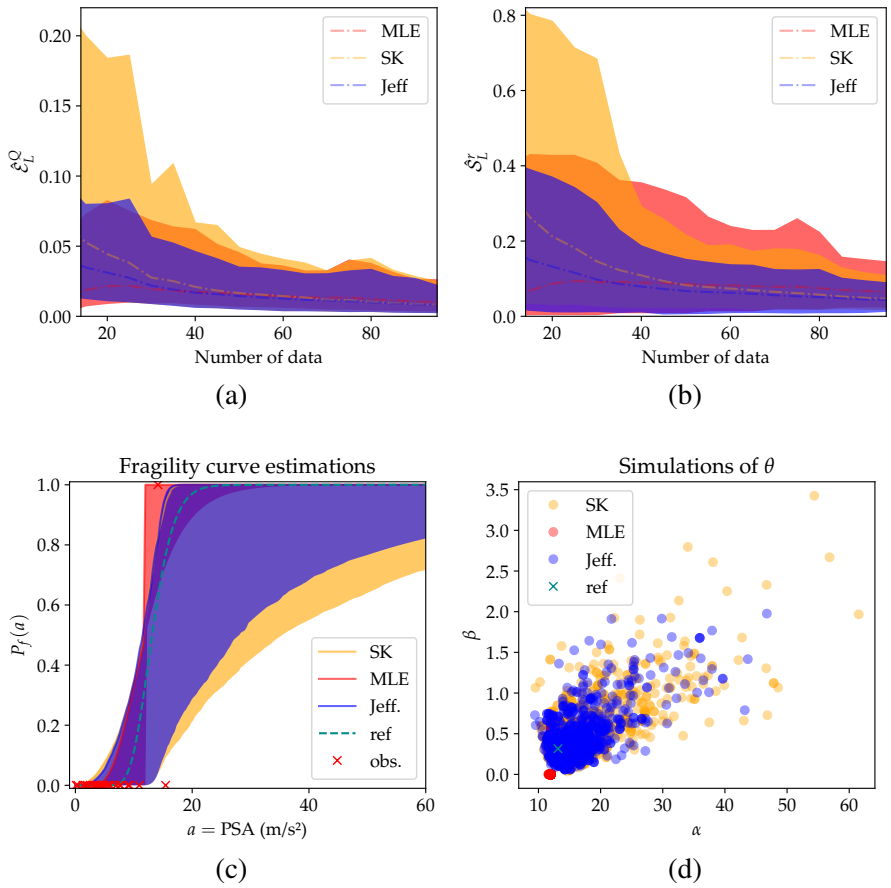

Figure 8: Same as in figure 7, but here the PSA is used as IM.

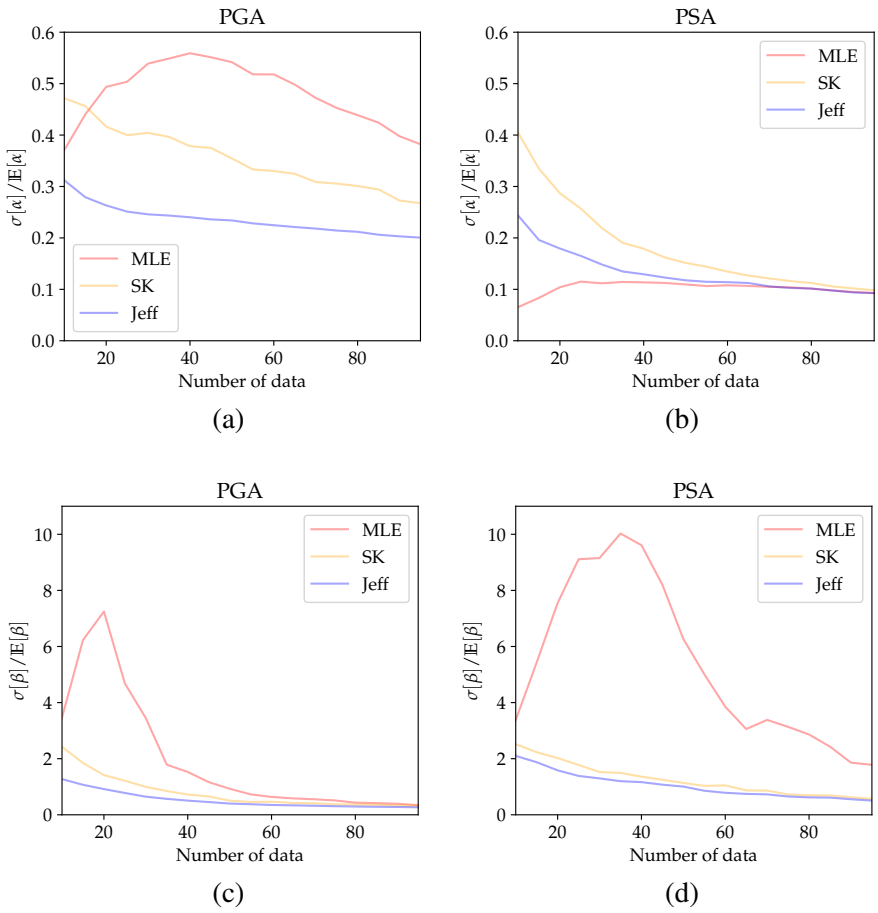

Figure 9: Average coefficient of variation of α (a-b) and of β (c-d) for the PGA and the PSA. For each value of k, 200 samples of size k have been used to compute the average values of the resulting 200 coefficients of variation from 5000 estimates of θ each.

7 Conclusion

Assessing the seismic fragility of Structures and Components when little data is available is a daunting task. The Bayesian framework is known to be efficient for this kind of problems. Nevertheless, the choice of the prior remains tricky because it has a non-negligible influence on the *a posteriori* distribution and therefore on the estimation of any quantity of interest linked to the fragility curves.

Using the reference prior theory to define an objective prior, we have derived the Jeffreys' prior for the log-normal model with binary data which indicate the state of the structure (e.g. failure or non-failure). In doing so, this prior is completely defined, it does not depend on an additional subjective choice.

Since this prior depends only on the characteristics of the ground motion – the distribution of the IM of interest – its calculation is then suitable for any equipment of an industrial installation subjected to the same seismic hazard. So, in this work, we were interested in the influence of the choice of the IM – PGA vs. PSA – on the convergence of the estimates, for a given (M,R) seismic scenario and a given mechanical structure, namely a piping system.

The results show, as expected, that when the IM is more correlated with the structural response, the differences between methods are less marked, although in detail there may be some small differences depending on sample size, due to possible degenerate samples. Theses results testify to the fact that an IM more correlated to the response of the structure essentially induces a lower variability of the estimate of the median of the log-normal model. This is not the case for the log standard deviation whose estimate is affected by samples which are more degenerate with this kind of IM. Such degeneracy affects all methods, however, in all cases, the Jeffreys' prior outperforms the classical approaches of the literature both in terms of regularization (absence of degenerate estimation) and stability (absence of outliers when sampling the *a posteriori* distribution of the parameters).

8 Acknowledgments

This research was supported by CEA (French Alternative Energies and Atomic Energy Commission) and SEISM Institute (www.institut-seism.fr/en/).

References

[1] Robert P. Kennedy, C. Allin Cornell, Robert D. Campbell, Stan J. Kaplan, and Harold F. Perla. Probabilistic seismic safety study of an existing nuclear power plant. *Nuclear Engineering and Design*, 59(2):315–338, 1980. ISSN 0029-5493. doi: 10.1016/0029-5493(80)90203-4.

[2] Robert P. Kennedy and Mayasandra K. Ravindra. Seismic fragilities for nuclear power plant risk studies. *Nuclear Engineering and Design*, 79(1):47–68, 1984. doi: 10.1016/0029-5493(84)90188-2.

[3] Young-Ji Park, Charles H. Hofmayer, and Nilesh C. Chokshi. Survey of seismic fragilities used in PRA studies of nuclear power plants. *Reliability Engineering & System Safety*, 62 (3):185–195, 1998. ISSN 0951-8320. doi: 10.1016/S0951-8320(98)00019-2.

[4] Robert P. Kennedy. Risk based seismic design criteria. *Nuclear Engineering and Design*, 192(2):117–135, 1999. ISSN 0029-5493. doi: 10.1016/S0029-5493(99)00102-8.

[5] C. Allin Cornell. Hazard, ground motions and probabilistic assessments for PBSD. In *Proceedings of the International Workshop on Performance-Based Seismic Design - Concepts and Implementation*, pages 39–52, University of California, Berkeley, 2004. PEER Center.

[6] Irmela Zentner, Max Gündel, and Nicolas Bonfils. Fragility analysis methods: Review of existing approaches and application. *Nuclear Engineering and Design*, 323:245–258, 11 2017. doi: 10.1016/j.nucengdes.2016.12.021.

[7] Paolo Gardoni, Armen Der Kiureghian, and Khalid M. Mosalam. Probabilistic capacity models and fragility estimates for reinforced concrete columns based on experimental observations. *Journal of Engineering Mechanics*, 128(10):1024–1038, 2002. doi: 10.1061/(ASCE)0733-9399(2002)128:10(1024).

[8] Do-Eun Choe, Paolo Gardoni, and David Rosowsky. Closed-form fragility estimates, parameter sensitivity, and bayesian updating for rc columns. *Journal of Engineering Mechanics*, 133(7):833–843, 2007. doi: 10.1061/(ASCE)0733-9399(2007)133:7(833).

[9] Masanobu Shinozuka, Maria Qing Feng, Jongheon Lee, and Toshihiko Naganuma. Statistical analysis of fragility curves. *Journal of Engineering Mechanics*, 126(12):1224–1231, 2000. doi: 10.1061/(ASCE)0733-9399(2000)126:12(1224).

[10] David Lallemant, Anne Kiremidjian, and Henry Burton. Statistical procedures for developing earthquake damage fragility curves. *Earthquake Engineering & Structural Dynamics*, 44(9):1373–1389, 2015. doi: 10.1002/eqe.2522.

[11] Daniel Straub and Armen Der Kiureghian. Improved seismic fragility modeling from empirical data. *Structural Safety*, 30(4):320–336, 07 2008. doi: 10.1016/j.strusafe.2007.05.004.

[12] Irmela Zentner. Numerical computation of fragility curves for NPP equipment. *Nuclear Engineering and Design*, 240(6):1614–1621, 2010. ISSN 0029-5493. doi: 10.1016/j.nucengdes.2010.02.030.

[13] Fan Wang and Cyril Feau. Influence of Input Motion's Control Point Location in Nonlinear SSI Analysis of Equipment Seismic Fragilities: Case Study on the Kashiwazaki-Kariwa NPP. *Pure and Applied Geophysics*, 2020. ISSN 1420-9136. doi: 10.1016/j.engstruct.2018.02.024.

[14] Tushar K. Mandal, Siddhartha Ghosh, and Nikil N. Pujari. Seismic fragility analysis of a typical indian PHWR containment: Comparison of fragility models. *Structural Safety*, 58:11–19, 2016. ISSN 0167-4730. doi: 10.1016/j.strusafe.2015.08.003.

[15] Zhiyi Wang, Nicola Pedroni, Irmela Zentner, and Enrico Zio. Seismic fragility analysis with artificial neural networks: Application to nuclear power plant equipment. *Engineering Structures*, 162:213–225, 2018. ISSN 0141-0296. doi: 10.1016/j.engstruct.2018.02.024.

[16] Zhiyi Wang, Irmela Zentner, and Enrico Zio. A Bayesian framework for estimating fragility curves based on seismic damage data and numerical simulations by adaptive neural networks. *Nuclear Engineering and Design*, 338:232–246, 2018. ISSN 0029-5493. doi: 10.1016/j.nucengdes.2018.08.016.

[17] Chnfeng Zhao, Na Yu, and Yilung Mo. Seismic fragility analysis of AP1000 SB considering fluid-structure interaction effects. *Structures*, 23:103–110, 2020. ISSN 2352-0124. doi: 10.1016/j.istruc.2019.11.003.

[18] Bruce R. Ellingwood. Earthquake risk assessment of building structures. *Reliability Engineering & System Safety*, 74(3):251–262, 2001. ISSN 0951-8320. doi: 10.1016/S0951-8320(01)00105-3.

[19] Sang-Hoon Kim and Masanobu Shinozuka. Development of fragility curves of bridges retrofitted by column jacketing. *Probabilistic Engineering Mechanics*, 19(1):105–112, 2004. ISSN 0266-8920. doi: 10.1016/j.probengmech.2003.11.009. Fourth International Conference on Computational Stochastic Mechanics.

[20] Chu Mai, Katerina Konakli, and Bruno Sudret. Seismic fragility curves for structures using non-parametric representations. *Frontiers of Structural and Civil Engineering*, 11 (2):169–186, 04 2017. doi: 10.1007/s11709-017-0385-y.

[21] Konstantinos Trevlopoulos, Cyril Feau, and Irmela Zentner. Parametric models averaging for optimized non-parametric fragility curve estimation based on intensity measure data clustering. *Structural Safety*, 81:101865, 2019. doi: 10.1016/j.strusafe.2019.05.002.

[22] Yoshifumi Katayama, Yasuki Ohtori, Toshiaki Sakai, and Hitoshi Muta. Bayesian-estimation-based method for generating fragility curves for high-fidelity seismic probability risk assessment. *Journal of Nuclear Science and Technology*, 58(11):1220–1234, 2021. doi: 10.1080/00223131.2021.1931517.

[23] P. Steve Koutsourelakis. Assessing structural vulnerability against earthquakes using multi-dimensional fragility surfaces: A Bayesian framework. *Probabilistic Engineering Mechanics*, 25(1):49–60, 2010. ISSN 0266-8920. doi: 10.1016/j.probengmech.2009.05.005.

[24] Guillaume Damblin, Merlin Keller, Alberto Pasanisi, Pierre Barbillon, and Éric Parent. Approche décisionnelle bayésienne pour estimer une courbe de fragilité. *Journal de la Societe Française de Statistique*, 155(3):78–103, 2014.

[25] Sashi Kanth Tadinada and Abhinav Gupta. Structural fragility of t-joint connections in large-scale piping systems using equivalent elastic time-history simulations. *Structural Safety*, 65:49–59, 2017. ISSN 0167-4730. doi: 10.1016/j.strusafe.2016.12.003.

[26] Shinyoung Kwag and Abhinav Gupta. Computationally efficient fragility assessment using equivalent elastic limit state and Bayesian updating. *Computers & Structures*, 197:1–11, 2018. ISSN 0045-7949. doi: 10.1016/j.compstruc.2017.11.011.

[27] Jong-Su Jeon, Sujith Mangalathu, Junho Song, and Reginald Desroches. Parameterized seismic fragility curves for curved multi-frame concrete box-girder bridges using bayesian parameter estimation. *Journal of Earthquake Engineering*, 23(6):954–979, 2019. doi: 10.1080/13632469.2017.1342291.

[28] Armin Tabandeh, Pouyan Asem, and Paolo Gardoni. Physics-based probabilistic models: Integrating differential equations and observational data. *Structural Safety*, 87:101981, 2020. ISSN 0167-4730. doi: 10.1016/j.strusafe.2020.101981.

[29] Antoine Van Biesbroeck, Clement Gauchy, Cyril Feau, and Josselin Garnier. Reference prior for bayesian estimation of seismic fragility curves. 2023. doi: 10.48550/ARXIV.2302.06935.

[30] Christian Robert. *The Bayesian Choice*. Texts in Statistics. Springer, 2 edition, 2007. ISBN 978-0-387-95231-4.

[31] José M. Bernardo. Reference posterior distributions for Bayesian inference. *Journal of the Royal Statistical Society. Series B*, 41(2):113–147, 01 1979. doi: 10.1111/j.2517-6161.1979.tb01066.x.

[32] James O. Berger, José M. Bernardo, and Dongchu Sun. The formal definition of reference priors. *The Annals of statistics*, 37(2):905–938, 05 2009. doi: 10.1214/07-AOS587.

[33] Bertrand S. Clarke and Andrew R. Barron. Jeffreys' prior is asymptotically least favorable under entropy risk. *Journal of Statistical Planning and Inference*, 41(1):37–60, 08 1994. doi: 10.1016/0378-3758(94)90153-8.

[34] José M. Bernardo. Reference analysis. In *Bayesian Thinking*, volume 25 of *Handbook of Statistics*, pages 17–90. Elsevier, 2005. doi: 10.1016/S0169-7161(05)25002-2.

[35] Sanaz Rezaeian. *Stochastic Modeling and Simulation of Ground Motions for Performance-Based Earthquake Engineering*. PhD thesis, University of California, Berkeley, 2010.

[36] Rémi Sainct, Cyril Feau, Jean-Marc Martinez, and Josselin Garnier. Efficient methodology for seismic fragility curves estimation by active learning on support vector machines. *Structural Safety*, 86:101972, 2020. doi: 10.1016/j.strusafe.2020.101972.

[37] Heikki Haario, Eero Saksman, and Johanna Tamminen. An adaptive metropolis algorithm. *Bernoulli*, 7(2):223–242, 04 2001. doi: 10.2307/3318737.

[38] Pierre Gehl, John Douglas, and Darius M. Seyedi. Influence of the number of dynamic analyses on the accuracy of structural response estimates. *Earthquake Spectra*, 31(1):97–113, 02 2015. doi: 10.1193/102912EQS320M.

[39] Jack W. Baker. Efficient analytical fragility function fitting using dynamic structural analysis. *Earthquake Spectra*, 31(1):579–599, 02 2015. doi: 10.1193/021113EQS025M.

[40] Aad van der Vaart. *Asymptotic statistics*. Cambridge Series in Statistical and Probabilistic Mathematics. Cambridge University Press, 1 edition, 1992. ISBN 9780511802256.

[41] Françoise Touboul, Pierre Sollogoub, and Nadine Blay. Seismic behaviour of piping systems with and without defects: experimental and numerical evaluations. *Nuclear Engineering and Design*, 192(2):243–260, 1999. ISSN 0029-5493. doi: 10.1016/S0029-5493(99)00111-9.

[42] CEA. CAST3M, 2019. URL http://www-cast3m.cea.fr/.

[43] Françoise Touboul, Nadine Blay, Pierre Sollogoub, and Stéphane Chapuliot. Enhanced seismic criteria for piping. *Nuclear Engineering and Design*, 236(1):1–9, 2006. ISSN 0029-5493. doi: 10.1016/j.nucengdes.2005.07.002.